HOKKAIDO UNIVERSITY

Title	Alendronate inhibits bone-specific blood vessels in the femoral metaphyses of mice
Author(s)	Hasegawa, Tomoka; Sakakibara, Mako; Liu, Xuanyu et al.
Citation	Journal of oral biosciences, 67(2), 100655 https://doi.org/10.1016/j.job.2025.100655
Issue Date	2025-03-19
Doc URL	https://hdl.handle.net/2115/97811
Rights	©2025. This manuscript version is made available under the CC-BY-NC-ND 4.0 license https://creativecommons.org/licenses/by-nc-nd/4.0/
Rights(URL)	https://creativecommons.org/licenses/by-nc-nd/4.0/
Type	journal article
File Information	2025.3.15._Hasegawa_revised_manuscript_JOB.pdf

Hokkaido University Collection of Scholarly and Academic Papers : HUSCAP

Alendronate inhibits bone-specific blood vessels in the femoral metaphyses of mice

Tomoka Hasegawa[1#§], Mako Sakakibara[1#], Xuanyu Liu[1#], Hirona Yoshino[1], Yan Shi[1], Jiaxin Cui[1], Mai Haraguchi-Kitakamae[1], Weisong Li[1], Wang Haoyu[1], Tomomaya Yamamoto[1,2], Hotaka Ishizu[1,3], Tamaki Sekiguchi[4], Tomohiro Shimizu[3], Norio Amizuka[1]

[1]Ultrastructure of Hard Tissue, Faculty of Dental Medicine, Hokkaido University, Sapporo, Japan, [2]Department of Dentistry, Japan Ground Self-Defense Force, Camp Shinmachi, Japan, [3]Orthopedic Surgery, Faculty of Medicine, Hokkaido University, Sapporo, Japan, [4]Oral and Maxillofacial Surgery, Faculty of Dental Medicine, Hokkaido University, Sapporo, Japan.

[#]***We regard these authors as having contributed equally***

Running title: Alendronate-treated blood vessels in bone

§ Corresponding Author

Tomoka Hasegawa, DDS, Ph.D.
Ultrastructure of Hard Tissue,
Graduate School of Dental Medicine,
Faculty of Dental Medicine, Hokkaido University
Kita 13, Nishi 7, Kita-Ku, Sapporo,
Hokkaido, 060-8586, Japan
Tel/fax: +81-11-706-4226
E-mail: hasegawa@den.hokudai.ac.jp

Abstract

To determine whether alendronate affects vascular endothelial cells and regulates the interactions between blood vessels and osteoblasts, we have examined the femoral metaphyses of alendronate-administered mice. Following administration, the bone-specific blood vessels exhibited significantly reduced luminal diameters and rough luminal surfaces with numerous small protrusions and vesicles. Although the osteoclast distribution remained unchanged in ALN-treated mice, osteoblasts were inactivated in the metaphyseal regions where blood vessels had shrunk. Additionally, the expression of genes such as *Ephb4*/*Efnb2*, which mediate vascular endothelial cell–osteoblast interactions, was diminished. Therefore, alendronate may primarily affect bone-specific blood vessels, thus leading to osteoblast inactivation.

98 words

***Keywords*:** Vascular endothelial cells, Alendronate, Osteoblast, Osteoclast, Endomucin

1. Introduction

Bone-specific blood vessels have been reported to be strongly positive for CD31 and endomucin [1,2]. Recent studies have demonstrated that endomucin-reactive bone-specific blood vessels promote osteogenesis via Notch signaling [2], and ephrinB2 signaling from osteoblasts induces angiogenesis [3]. We previously reported that endomucin-reactive bone-specific blood vessels express EphB4, indicating that these vessels are venous and sinusoidal, while osteoblasts located close to blood vessels express ephrinB2 [4]. Additionally, TEM observations revealed cell-to-cell contact between endothelial cells and osteoblasts [4], suggesting a potential interaction between endomucin/EphB4-reactive vascular endothelial cells and ephrinB2-positive osteoblasts. Expression of EphB4/ephrinB2 increased when murine femora were treated with human parathyroid hormone (1–34) [5,6], indicating that parathyroid hormone-driven interactions occur between osteoblasts and bone-specific blood vessels.

Alendronate (ALN), one of the most common bisphosphonates used for osteoporotic treatment, accumulates in the mineralized bone matrix. Osteoclasts resorb the bisphosphonates bound to crystalline calcium phosphates in the bone matrix through the ruffled border. Consequently, incorporated bisphosphonates inhibit osteoclasts by inducing apoptosis, which diminishes osteoblastic activity by disrupting cell coupling with osteoclasts [7,8]. Additionally, bisphosphonate treatments have been reported to cause anti-angiogenic effects in co-cultures of human dermal microvascular endothelial cells and human bone marrow mesenchymal stem cells [9], attenuate neovascularization [10], and produce a less connected and less ordered distribution of blood vessels in the mandible [11]. However, it is still not known whether the endomucin-positive bone-specific blood vessels surrounding metaphyseal trabeculae are affected by bisphosphonate or whether bisphosphonate diminishes interplay with nearby osteoblastic cells.

Therefore, to clarify whether ALN affects the vascular endothelial cells of bone-specific blood vessels and the expression of the molecules moderating interactions between these blood vessels and osteoblasts, we histochemically examined bone-specific blood vessels in the femoral metaphyses of ALN-administered mice.

2. Materials and methods

2.1. Animals and tissue preparation

Six-week-old male ICR mice (*n* = 12, Japan CLEA, Tokyo, Japan) were handled according to Hokkaido University's guidelines for animal care and research use (approved study protocol #20-0008). All mice received subcutaneous injections of the vehicle (phosphate-buffered saline; control group) or 1 mg/kg of alendronate (ALN group; FUJIFILM Wako Pure Chemical Corporation, Osaka, Japan) once a day for 10 days according to the methods described in our previous report [8].

After 10 days, under anesthetization using an intraperitoneal injection of a combination of anesthetic agents including 0.3 mg/kg of medetomidine, 4.0 mg/kg of midazolam, and 5.0 mg/kg of butorphanol, each mouse's left femora was surgically removed for RNA extraction, and then the mice were perfused with a 4% paraformaldehyde, 0.1 M phosphate buffer solution (pH 7.4). The right femora were decalcified in 10% ethylenediaminetetraacetic disodium salt for 2 months at 4 °C and then dissected into two pieces parallel to the sagittal plane. One piece was embedded in paraffin for histochemical examination and the other in epoxy resin for TEM (Hitachi 7800, Hitachi Co., Tokyo, Japan).

2.2. Double detection of TRAP/ALP and endomucin/ALP on histological sections

For the simultaneous detection of both endomucin and alkaline phosphatase (ALP), femoral sections were incubated with rat antibody to endomucin (Santa Cruz Biotecnology, Inc., Dallas, TX) and then with horseradish peroxidase-conjugated anti-rat IgG (Zymed Laboratories Inc., South San Francisco, CA), USAboth at 1:100 dilutions. Subsequently, the sections were incubated with rabbit polyclonal antiserum against ALP [12], at a dilution of 1:300, followed by ALP-conjugated anti-rabbit IgGs (Rockland Immunochemicals Inc., Gilbertsville, PA) at a 1:100 dilution. These sections were then immersed in 30 mL of a 0.1 M tris-HCl buffer (pH 8.5) containing 2.5 mg of naphthol AS-BI phosphate (Sigma-Aldrich, Saint Louis, MO) and 18 mg of fast blue RR salt (Sigma-Aldrich) for 15 min at 37 °C, making ALP-immunoreactivity visible, and double staining of tartrate-resistant acid phosphatase (TRAP)/ALP was conducted as previous described [13].

2.3. Regions of interest (ROIs) in metaphyses for measuring the number, average luminal diameter, and total area of blood vessels

An assumed 600 (width) × 1200 (height) μm rectangular area oriented perpendicular to the femur's longitudinal axis and positioned just below the growth plate and in the center of each femur was selected as the region of interest (ROI). In each ROI, the number of blood vessels, averaged luminal diameter of blood vessels, and total areas of blood vessels were analyzed as described in our previous report [5].

2.4. Quantitative analysis of gene expression related to vascular endothelial cells in bone

After collecting the left femora, total RNA was extracted from the samples and cDNA was generated as previously reported [14]. The relative expression levels of various genes were quantified via the ΔΔCt method, using *Gapdh* (Mm00468869_m1) as the reference gene, in a quantitative PCR System (StepOne; Thermo Fisher Scientific Inc., Waltham, MA, USA). Analyzed genes included *Acta2* (αSMA; Mm00725412_s1), *Alp* (Mm00475834_m1), *Cdh5* (VE-cadherin; Mm00486938_m1), *Dll4* (Mm00444619_m1), *Efnb2* (EphrinB2; Mm00438670_m1), *Emcn* (Endomucin; Mn00438980_m1), *Ephb4* (Mm99999915_g1), *Flt1* (Mm00492301_m1), *Gata2* (Mm00496902_m1), *Hif1a* (Mm01222421_m1), *Jag1* (Jagged1; Mm00627185_m1), *Kdr* (Mm00803077_m1), *Notch1* (Mm00440525_m1), *Notch2* (Mm00440677_m1), *Notch4* (Mm00437306_m1), *Pdgfb* (Mm01333430_m1), *Vegfa* (Mm00437306_m1), *Vim* (Vimentin; Mm01333430_m1). TaqMan probes (Applied Biosystems, Waltham, MA, USA) were used for this analysis.

2.5. Statistical analysis

All values are presented as means ± standard deviations (SDs). Student's *t*-tests were used for comparisons between the two treatment groups. For all tests, P-values < 0.05 were considered significant.

3. Results and discussion

In ALN-administrated mice, the numbers of trabeculae in the femora were slightly increased compared to control mice **(Fig. 1A** and **D)**. The femoral metaphyses of control mice showed many large endomucin-immunoreactive blood vessels, whereas those of the ALN-treated mice contained markedly small endomucin-positive blood vessels **(Fig. 1B** and **E)**. Semi-thin section demonstrated thin luminal walls with smooth surfaces in the blood vessels of the metaphyses of control mice, while relatively thick walls were observed in the ALN-treated mice's small blood vessels **(Fig. 1C** and **F)**. The numbers of endomucin-immunoreactive blood vessels were not significantly different, but the luminal areas and diameters of endomucin-positive blood vessels were significantly reduced in the metaphyses of ALN-administrated mice **(Fig. 1G–I)**.

We compared the localization of TRAP-positive osteoclasts, ALP-reactive osteoblasts, and endomucin-positive blood vessels **(Fig. 2A–H)**. After ALN administration, the distribution pattern of TRAP-positive osteoclasts did not seem to differ between the control and ALN-treated mice **(Fig. 2A**, **B**, **E**, and **F)**; Therefore, a 1 mg/kg, 10-day regimen of ALN is not enough to completely inhibit osteoclasts. However, ALN-treated mice did not exhibit ALP-reactive osteoblasts on metaphyseal trabeculae close to the diaphysis **(Fig. 2 C–H)**. Double detection of ALP and endomucin immunoreactivity demonstrated a broad distribution of ALP-positive osteoblasts in the control specimens, while ALP-positive areas were primarily seen close to the chondro–osseous junction in the ALN-treated mice **(Fig. 2C** and **D)**. In the region of the metaphysis close to the diaphysis, where the endomucin-positive blood vessels were shrunken, few ALP-reactive osteoblasts were seen in the ALN-treated mice **(Fig. 2G** and **H)**. Thus, despite the presence of osteoclasts, osteoblasts beside the shrunken endomucin-positive blood vessels seemed to be inhibited, demonstrating little or no ALP activity.

The TEM imaging verified that the luminal walls of the vascular endothelial cells of control mice had smooth surfaces **(Fig. 2I** and **K)**. However, in ALN-treated mice, vascular endothelial cells showed rough luminal surfaces, often with extended short protrusions from the luminal cell membrane **(Fig. 2J** and **L)**, and many small vesicles

accumulated on the luminal walls of the vascular endothelial cells **(Fig. 2M** and **N)**. Therefore, ALN appears to affect vascular endothelial cells by reducing the luminal size and producing many cytoplasmic protrusions and vesicles.

We attempted to verify the expression of genes associated with angiogenesis, the maintenance of the vasculature, and interactions between vascular endothelial cells and osteoblasts. The genes *Vegfa, Flt1, Kdr, Endomucin*, factors for angiogenesis and vascular maintenance, as well as *Ephb4/Efnb2* and *Notch4/Dll4* [2–5], which mediate interactions between osteoblasts and blood vessels, were significantly reduced in the ALN-treated mice **(Fig. 3)**. Taken together, it is possible that ALN inhibits endomucin-positive vascular endothelial cells, reducing osteoblastic activity.

Conclusion

Alendronate administration resulted in small, shrunken, and irregularly shaped endomucin-positive blood vessels with small protrusions from the vascular endothelial cells in the metaphysis. After ALN administration, the inhibition of the osteoblasts appears to be consistent with the decreased size of bone-specific blood vessels rather than osteoclastic inhibition.

Ethical standards

All animal experiments were performed in accordance with the Japanese Act on the Welfare and Management of Animals. The protocol was approved by the Institutional Animal Care and Use Committee of Hokkaido University (approved research proposal #20-0008).

Competing interests

The authors declare no competing interests.

Author contributions

Hasegawa T designed this study and prepared the final draft of the article. We regard Hasegawa T, Sakakibara M, and Liu X as first authors in charge of writing the original draft and interpreting the data. Yoshino H performed mainly histochemistry analyses with the assistance of Shi Y, Cui J, Haraguchi-Kitakamae M, Li W, Wang H, Yamamoto T, Ishizu H, and Sekiguchi T contributed to the gene expression and statistical analyses. Shimizu T and Amizuka N participated in the discussion, editing, and formatting of the manuscript.

Funding statement

This study was partially supported by grants from the Japan Society for the Promotion of Science (JSPS, 24K02609 to Amizuka N, 23K09114 to Sekiguchi T).

References

1. Kusumbe AP, Ramasamy SK, Adams RH. Coupling of angiogenesis and osteogenesis by a specific vessel subtype in bone. ***Nature***. 507: 323-328, 2014.

2. Ramasamy SK, Kusumbe AP, Wang L, Adams RH. Endothelial Notch activity promotes angiogenesis and osteogenesis in bone. ***Nature.*** 507: 376-380, 2014.

3. Qu F, Shen YY, Zhang XY, Wu YQ, Xu ZH, Zhai ZD, et al. Ephrin-B2 acts as a positive regulator of osteogenesis-angiogenesis coupling. ***Int J Biol Macromol.*** 2025. Online ahead of print.

4. Tsuchiya E, Hasegawa T, Hongo H, Yamamoto T, Abe M, Yoshida T, et al. Histochemical assessment on the cellular interplay of vascular endothelial cells and septoclasts during endochondral ossification in mice. ***Microscopy (Oxf).*** 70(2): 201-214, 2021.

5. Zhao S, Hasegawa T, Hongo H, Yamamoto T, Abe M, Yoshida T, et al. Intermittent PTH administration increases bone-specific blood vessels and surrounding stromal cells in murine long bones. ***Calcif Tissue Int.*** 108: 391-406, 2021.

6. Maruoka H, Zhao S, Yoshino H, Abe M, Yamamoto T, Hongo H, et al. Histochemical examination of blood vessels in murine femora with intermittent PTH administration. ***J Oral Biosci.*** 64(3): 329-336, 2022.

7. Azuma Y, Sato H, Oue Y, Okabe K, Ohta T, Tsuchimoto M, et al. Alendronate distributed on bone surfaces inhibits osteoclastic bone resorption in vitro and in experimental hypercalcemia models. ***Bone.*** 16(2): 235-245, 1995.

8. Tsuboi K, Hasegawa T, Yamamoto T, Sasaki M, Hongo H, de Freitas PH, et al. Effects of drug discontinuation after short-term daily alendronate administration on osteoblasts and osteocytes in mice. ***Histochem Cell Biol.*** 146(3): 337-350, 2016.

9. Ribeiro V, Garcia M, Oliveira R, Gomes PS, Colaço B, Fernandes MH. Bisphosphonates induce the osteogenic gene expression in co-cultured human endothelial and mesenchymal stem cells. ***J Cell Mol Med.*** 18(1): 27-37, 2014.

10. Yang JX, Chen B, Pan YY, Han J, Chen F, Hu SJ. Zoledronate attenuates angiogenic effects of angiotensin II-stimulated endothelial progenitor cells via RhoA and MAPK signaling. ***PLoS One.*** 7(10): e46511, 2012.

11. Guevarra CS, Borke JL, Stevens MR, Bisch FC, Zakhary I, Messer R, et al. Vascular alterations in the sprague-dawley rat mandible during intravenous bisphosphonate therapy. ***J Oral Implantol.*** 41(2): e24-29, 2015.

12. Oda K, Amaya Y, Fukushi-Irié M, Kinameri Y, Ohsuye K, Kubota I, et al. A general method for rapid purification of soluble versions of glycosylphosphatidylinositol-anchored proteins expressed in insect cells: an application for human tissue-nonspecific alkaline phosphatase. ***J Biochem.*** 126(4): 694-699, 1999.

13. Hongo H, Sasaki M, Kobayashi S, Hasegawa T, Yamamoto T, Tsuboi K, et al. Localization of minodronate in mouse femora through isotope microscopy. ***J Histochem Cytochem.*** 64(10): 601-622, 2016.

289 **14.** Hasegawa T, Tokunaga S, Yamamoto T, Sakai M, Hongo H, Kawata T, et al.
290 Evocalcet rescues secondary hyperparathyroidism-driven cortical porosity in CKD
291 male rats. ***Endocrinology.*** 164(4): bqad022, 2023.

Figure Legends

Fig. 1. Histology of bone-specific blood vessels with and without ALN administration Panels **A** and **D** show the whole femoral metaphyses of the control (**A**) and the ALN-treated (**D**) mice. Endomucin-immunoreactive blood vessels (brown color and "BV" labels in **B** and **E**) were numerous and large in the femoral metaphyses of control mice, while in the ALN-treated mice, endomucin-positive blood vessels were markedly small (arrows in **E**). Toluidine blue-stained semithin sections (**C** and **D**) reveal thin blood vessel walls in the control specimens (arrow in **C**), but stout walls with rough surfaces in the ALN-treated specimens (arrows in **F**). The bar graphs show the number of blood vessels (**G**), the average index of lumina diameter of blood vessels (**H**), and the total area per blood vessel (**I**). All values are presented as means ± SDs, and statistical analysis results are shown above the bars. epi: epiphysis, GP: growth plate, meta: metaphysis

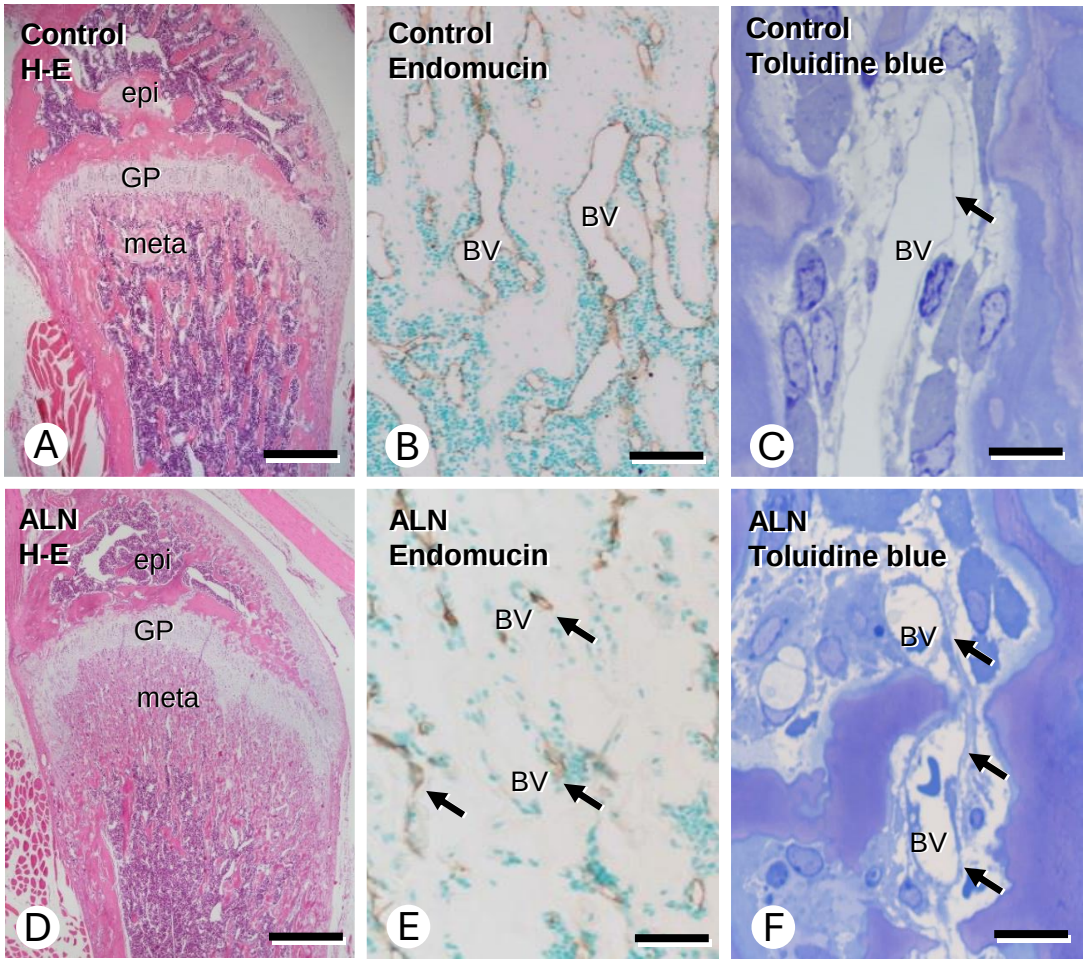
Bars, A, D: 900μm, B, E: 200 μm, C, F: 10 μm

Fig. 2. Histochemistry and ultrastructure of bone-specific blood vessels with and without ALN administration Panels **A**, **C**, **E**, and **G** are derived from the metaphyses of control mice, while panels **B**, **D**, **F**, and **H** show those of ALN-treated mice. Panels **E–H** are highly magnified images of **A–D**. Double detection of TRAP and ALP identified both TRAP-positive osteoclasts (red color, "oc") and ALP-reactive osteoblasts (brown color, arrows) in the control specimens (**E**), but no ALP-reactive osteoblasts were found in the ALN-treated specimen (**F**) despite the presence of osteoclasts. Dual immunostaining of endomucin (brown) and ALP (purple) demonstrated that ALP-positive osteoblasts are broadly present in the metaphyses of control mice (**C**) but restricted to the chondro–osseous junction in the ALN-treated mice(**D**). Red arrows indicating the osteoblastic distribution were added at the right of panels **C** and **D** to facilitate comparison between the ALN-treated and control mice. At higher magnifications, it is clear that ALP-positive osteoblasts (black arrows) accumulate on the trabecular bones (TB) neighboring large blood vessels (BV, white arrowheads) in the control specimen (**G**). However, no ALP-positive cells are seen on the trabecular bones

in the ALN-treated specimens, and shrunken blood vessels (BV, white arrowheads) are seen in the vicinity of the trabeculae (**H**). The TEM images demonstrate the smooth surfaces of blood vessels in control mice (**I**), and the rough surfaces of the ALN-treated mice's blood vessels (**J**). At a higher magnification, short cytoplasmic processes expanding from the luminal cell membranes are apparent in the blood vessels of ALN-treated mice (arrowheads, **L**), but not in those of the control mice(**K**). In the blood vessels of ALN-treated mice (**M** and **N**), there are many small vesicles inside the lumen (arrowheads, **N**).

Bars, A-D: 400μm, E-H: 100 μm, I, J: 10 μm, K, L: 2 μm, M: 5 μm, N: 1 μm

Fig. 3. Quantitative PCR analysis of the expression of genes related to angiogenesis and interactions between blood vessels and osteoblastic cells Quantitative PCR demonstrated significant reductions in the expression of *Emun* (endomucin), *Ephb4, Efnb2* (ephrinB2), *Vefga*, *Flt1*(VEGFR1), *Kdr* (VEGFR2), *Alp*, *Notch4*, *Dll4*, *Jag1*(Jagged1), and *Cdh5*(VE-cadherin) in ALN-treated mice (**A–K**), but increases in *Notch2* and *Gata2* expression (**L** and **M**). There was no significant difference between control and ALN-treated mice in the expression of *Vim* (Vimentin), *Notch1*, *Acta2* (αSMA), *Pdgfb*, or *Hif1α* (**N–R**).


Control
H-E
epi
GP
meta
A
Control
Endomucin
BV
BV
B
Control
Toluidine blue
BV
C
ALN
H-E
epi
GP
meta
D
ALN
Endomucin
BV
BV
E
ALN
Toluidine blue
BV
BV
F

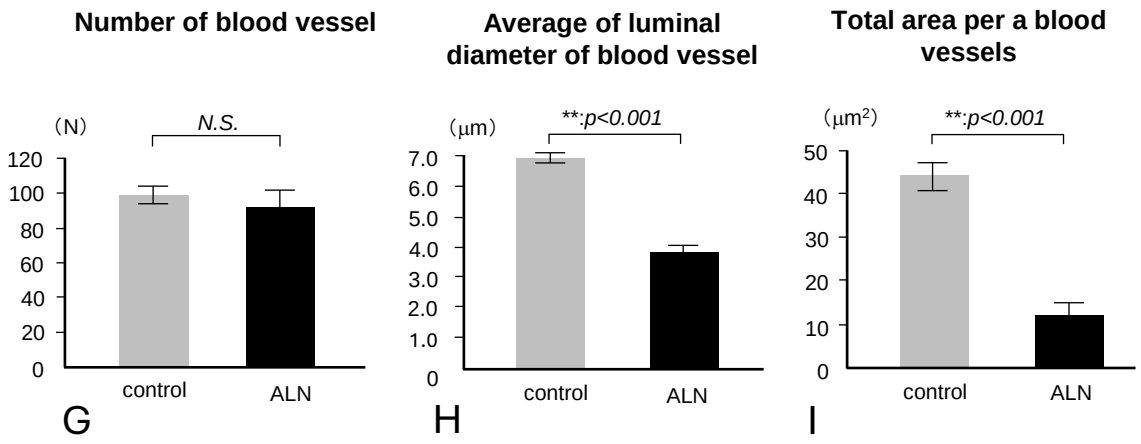

Number of blood vessel
(N)
N.S.
120
100
80
60
40
20
0
control
ALN
G
Average of luminal diameter of blood vessel
(μm)
**:p<0.001
7.0
6.0
5.0
4.0
3.0
2.0
1.0
0
control
ALN
H
Total area per a blood vessels
(μm²)
**:p<0.001
50
40
30
20
10
0
control
ALN
I

Figure.1

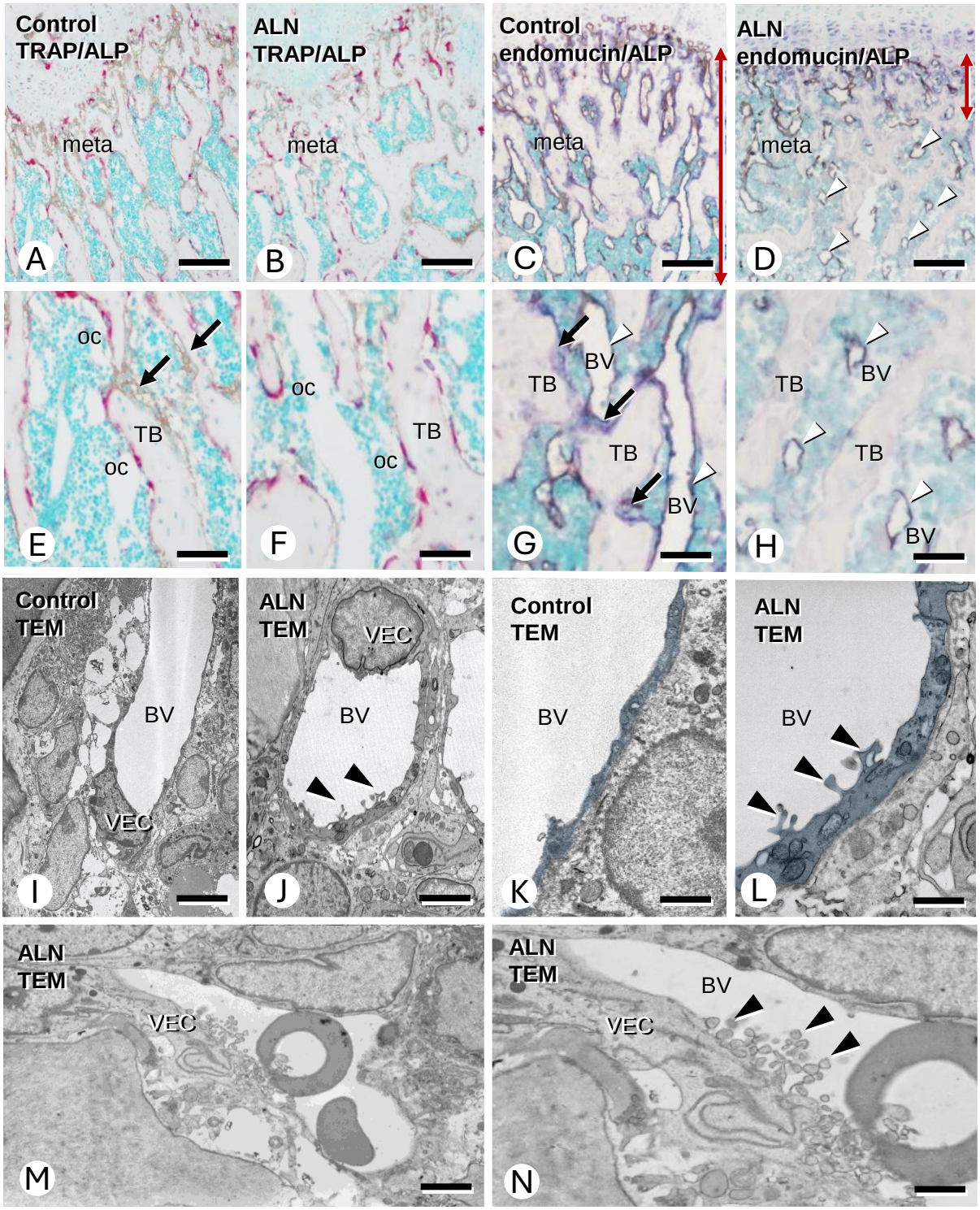

Control
TRAP/ALP
meta
A
ALN
TRAP/ALP
meta
B
Control
endomucin/ALP
meta
C
ALN
endomucin/ALP
meta
D
oc
TB
oc
E
oc
TB
oc
F
BV
TB
TB
BV
G
TB
BV
TB
BV
H
Control
TEM
BV
VEC
I
ALN
TEM
VEC
BV
J
Control
TEM
BV
K
ALN
TEM
BV
L
ALN
TEM
VEC
M
ALN
TEM
BV
VEC
N

Figure.2

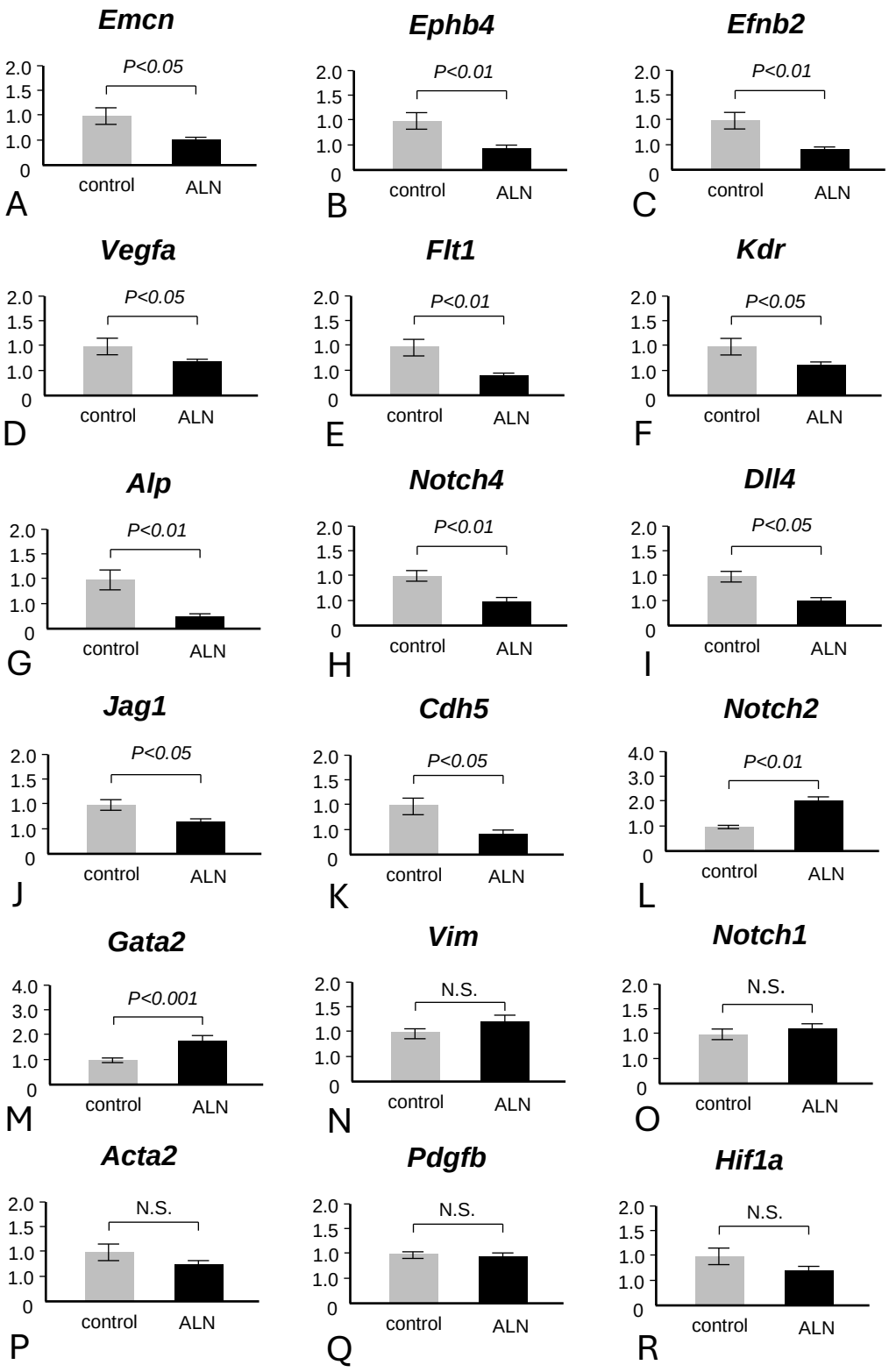

Emcn
P<0.05
control
ALN
A
Ephb4
P<0.01
B
Efnb2
P<0.01
C
Vegfa
P<0.05
D
Flt1
P<0.01
E
Kdr
P<0.05
F
Alp
P<0.01
G
Notch4
P<0.01
H
Dll4
P<0.05
I
Jag1
P<0.05
J
Cdh5
P<0.05
K
Notch2
P<0.01
L
Gata2
P<0.001
M
Vim
N.S.
N
Notch1
N.S.
O
Acta2
N.S.
P
Pdgfb
N.S.
Q
Hif1a
N.S.
R

Figure.3